A Nonreciprocal CRLH Full-Duplex Metamaterial Leaky Wave Antenna Based on Distributed Mixing Principle

Shaghayegh Vosoughitabar, *Graduate Student Member, IEEE*, Minning Zhu, *Member, IEEE*, Alireza Nooraiepour, and Chung-Tse Michael Wu, *Senior Member, IEEE*

***Abstract*— A new type of nonreciprocal composite right/left-handed leaky wave antenna (CRLH LWA) is introduced, which incorporates a distributed mixer (DM) for simultaneous transmit and receive. In this proposed design, the drain line of the DM is formed by the CRLH LWA, while the gate line consists of a conventional microstrip line. GaAs-based field-effect transistors (FETs) are used as mixing elements within the microstrip line. The local oscillator (LO) signal is injected through the input port of the microstrip line, connected to the FET gates. In the receive mode, the RF signal captured by the CRLH LWA on the drain side propagates in the same direction as the LO signal. Conversely, during the transmit mode, the RF signal is injected from the composite right/left-handed (CRLH) drain line port in the opposite direction to the LO signal. By leveraging the principles of the DM, it is demonstrated both theoretically and through measurements that the proposed CRLH DM exhibits a directional dependency in its mixing behavior. This characteristic allows for good isolation between the transmit and receive modes for the intermediate frequency (IF) signal by selecting an appropriate IF signal extracted from the other port of the CRLH drain line. This directional dependency in RF-to-IF conversion, which exhibits nonreciprocal property, provided by the CRLH DM enables simultaneous transmission and reception of the RF signal. The received information can be extracted from the downconverted IF signal.**

***Index Terms*— Composite right/left-handed-transmission lines (CRLH TLs), distributed mixers (DMs), leaky wave antennas (LWAs), nonreciprocal, simultaneous transmit and receive.**

I. Introduction

DISTRIBUTED mixers (DMs) based on traveling wave propagation along nonlinearly coupled transmission lines (TLs) offer the advantage of wideband mixing performance, thanks to the nature of the distributed network [1], [2]. This topology has been implemented in both complementary metal–oxide–semiconductor (CMOS) and monolithic microwave integrated circuits (MMICs) for microwave and millimeter-wave applications [3], [4]. On the other hand, composite right/left-handed (CRLH) unit cells, which exhibit properties such as negative phase velocity and propagation constant, are used in designing antennas for various wireless communication applications [5], [6], [7], [8]. In this regard, CRLH TL-based distributed circuits are integrated into the design of DMs to achieve novel functionalities, such as dual-band mixing behavior and wideband image rejection capability [9], [10], [11]. Furthermore, these CRLH TL-based circuits can be implemented in distributed amplifiers for both guided and radiated-wave applications, enabling the realization of multiband amplifiers and active antennas [12], [13], [14], [15], [16], [17], [18], [19].

Similar to the concept of DM, very recently, time-varying TLs incorporating time modulation as an additional degree of freedom for designing nonreciprocal components have been proposed in [20] and [21], in which balanced TLs are loaded with varactor diodes to realize time-modulated capacitance along the TL. In this case, the RF signal propagating in the same direction as the local oscillator (LO) signal will result in a maximal intermediate frequency (IF) downconversion, while the one traveling against the LO direction will exhibit much less signal conversion gain. Owing to the difference in the propagation directions of the transmit and receive signals, the direction-dependent conversion gain is leveraged to realize the signal isolation, and consequently nonreciprocity is achieved. Nevertheless, since three-port variable capacitors are either not available in practice or not sensitive enough to achieve high-capacitance modulation index, the time-varying TLs have been realized in a double-balanced fashion which quadruples the number of varactor diodes [20], [21]. Moreover, two pairs of differential TLs are used to carry the carrier wave and the signal wave separately, thereby increasing the design complexity.

While several nonreciprocal leaky wave antennas (LWAs) based on magnetically biased ferrite materials have been reported in the past decade [22], [23], [24], these ferrite-based components have inherent disadvantages such as bulkiness, heaviness, high cost, and limited compatibility with integrated circuit technologies, particularly at higher operating

Manuscript received 21 January 2024; revised 30 March 2024; accepted 10 May 2024. This work was supported in part by the National Science Foundation (NSF) under Grant ECCS-1818478, Grant ECCS-2028823, Grant ECCS-2033433, Grant CNS-2332637, Grant ECCS-2229384, and Grant CNS-2128077; and in part by the Ministry of Education (MOE), Taiwan, under Grant NTU-113V1042-1. This article is an expanded version from the IEEE MTT-S International Microwave Symposium (IMS 2021) [DOI: 10.1109/IMS19712.2021.9574840]. *(Corresponding author: Chung-Tse Michael Wu.)*

Shaghayegh Vosoughitabar and Minning Zhu are with the Department of Electrical and Computer Engineering, Rutgers University, New Brunswick, NJ 08854 USA (e-mail: sv600@scarletmail.rutgers.edu; mz368@scarletmail.rutgers.edu).

Alireza Nooraiepour is with Qualcomm, Inc., San Diego, CA 92121 USA (e-mail: anooraie@qti.qualcomm.com).

Chung-Tse Michael Wu is with the Department of Electrical and Computer Engineering, Rutgers University, New Brunswick, NJ 08854 USA, and also with the Department of Electrical Engineering, National Taiwan University, Taipei 10617, Taiwan (e-mail: ctmwu@ntu.edu.tw).

Color versions of one or more figures in this article are available at https://doi.org/10.1109/TMTT.2024.3401828.

Digital Object Identifier 10.1109/TMTT.2024.3401828

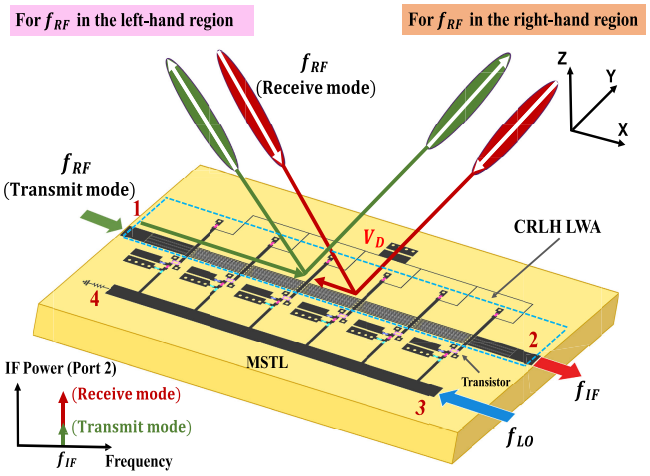

Fig. 1. Proposed nonreciprocal CRLH metamaterial LWA based on DM.

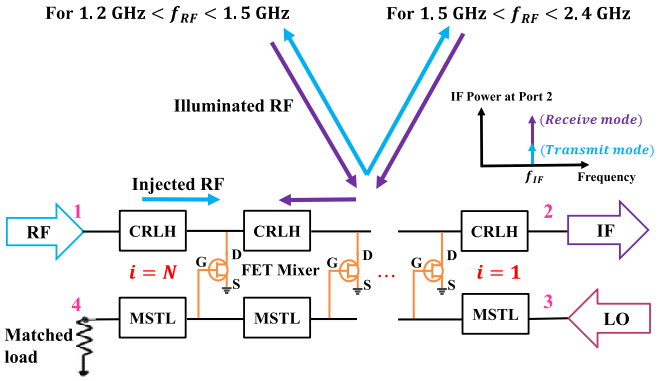

Fig. 2. Proposed nonreciprocal CRLH metamaterial LWA based on DM.

frequencies. As a result, recent efforts have been focused on developing nonreciprocal devices that do not rely on magnetic materials. For instance, in [25], a mixer–duplexer–antenna leaky wave system based on periodic space–time modulation is proposed. Nevertheless, in this approach, the signal is transmitted and received at the same carrier frequency, necessitating a large antenna aperture to achieve adequate isolation. Furthermore, due to the characteristics of conventional LWAs, only a limited scanning angle in the forward region is demonstrated.

To address these challenges, we present a new kind of nonreciprocal CRLH LWA for simultaneous transmit and receive, by leveraging the unique combination of CRLH LWA and DM using field-effect transistors (FETs) as mixing elements, as illustrated in Fig. 1. While we briefly introduce the basic principle in our previous work [26], this article significantly expands the theoretical analysis by deriving equations to explain the isolation of the downconverted IF signal between the transmit and receive modes. Moreover, to validate the proposed nonreciprocal mixing property of the proposed LWA, we conduct over-the-air (OTA) measurements in the receive mode by illuminating the signal from various directions in the far-field region of the CRLH LWA. In this case, the IF signal from Port 2 is collected to obtain the isolation between the transmit and receive modes. In addition, we conduct bit-error-rate (BER) measurements under both QPSK and 16QAM modulation schemes to investigate simultaneous transmit and receive operation in a real scenario. As depicted in Fig. 1, CRLH unit cells are connected to the drain of the FETs, while the LO signal is injected into the DM (Port 3) through a microstrip TL (MSTL) connected to the gates. In the receive mode, the RF signal received by the CRLH LWA propagates along the drain line in the same direction as the LO signal in the gate line. Conversely, in the transmit mode, the RF signal is injected from the CRLH drain line (Port 1) in the opposite direction to the LO signal in the gate line. When a propagating wave travels through a nonreciprocal medium, the interaction between the field and the system depends on the direction in which the wave travels through the medium. In the proposed design, the directional dependency in the mixing behavior results in significant isolation of the downconverted IF signal at Port 2 between the transmit and receive modes, thereby enabling simultaneous transmission and reception. This will be demonstrated through our analysis and measurements, as shown in Sections II–IV.

II. Operating Principles

A. Isolation Performance of DM-Based CRLH-LWA

The conventional DMs typically use two MSTLs connected to mixing components such as diodes or transistors to form frequency conversion [1]. In contrast to the conventional DMs where both RF and LO are injected to the gate side of an FET, in our proposed scheme shown in Fig. 2, the LO is injected from the gate, whereas the RF signal is injected from the drain CRLH TL in the transmit mode and is received by the LWA located in the drain side in the receive mode. When the signal is received by the CRLH LWA cells, it propagates toward Port 1, which is similar to the case where the RF signal is injected into Port 2. According to the method provided in [1] based on distributed mixing principle, the reverse conversion gain (G_{rev}) with respect to Port 2 can be calculated in terms of g_1 (conversion transconductance), $Z_{\pi d}$ (drain line impedance), β_g (gate line wavenumber), β_d (drain line wavenumber), and N (number of CRLH unit cells with a length of p) as follows:

$$G_{\text{rev}} = \frac{P_{\text{IF}}(\text{Port 2})}{P_{\text{RF}}} = \frac{g_1^2}{16} Z_{\pi d}(f_{\text{IF}}) Z_{\pi d}(f_{\text{RF}}) \left| \frac{\sin \frac{Np\theta_r}{2}}{\sin \frac{p\theta_r}{2}} \right|^2 \quad (1)$$

where in the transmit mode

$$\theta_r = \left| \beta_d(f_{\text{RF}}) + \beta_g(f_{\text{LO}}) \right| + \beta_d(f_{\text{IF}}) \quad (2)$$

and in the receive mode

$$\theta_r = \left| \beta_d(f_{\text{RF}}) - \beta_g(f_{\text{LO}}) \right| + \beta_d(f_{\text{IF}}). \quad (3)$$

From (1) and (3), the maximum reverse conversion gain G_{rev} is obtained when $\theta_r = 0$ in the receive mode at Port 2, as shown in Fig. 1. It can be seen that G_{rev} exhibits a sinc^2-type behavior. Therefore, by ensuring that $\theta_r = 0$ in the receive mode and $\theta_r \neq 0$ in the transmit mode (except when RF is around the center frequency where $\beta_d(f_{\text{RF}}) \approx 0$), we can anticipate good isolation.

An equivalent circuit model of a symmetric CRLH unit cell is shown in Fig. 3 including an RH inductance L_R in series

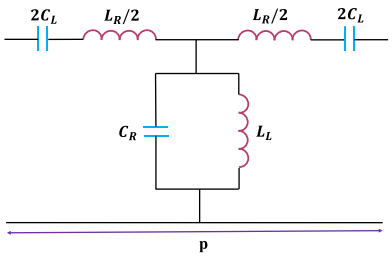

Fig. 3. Equivalent circuit model of a CRLH unit cell.

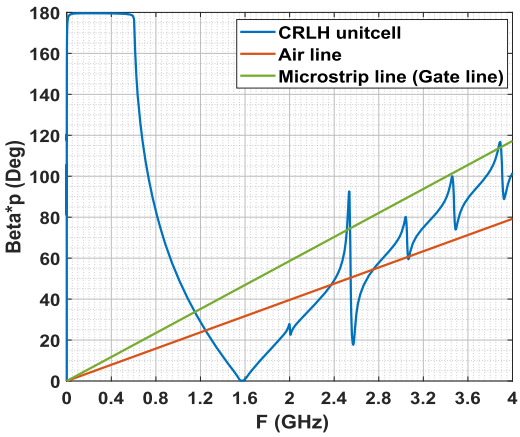

Fig. 4. Dispersion diagram of CRLH unit cell (drain), microstrip line (gate), and air line.

with an LH capacitance C_L and an RH capacitance C_R in parallel with an LH inductance L_L. The propagation constant β_d is calculated according to the dispersion diagram of an ideal CRLH TL with the unit cell length p using the following formula [27]:

$$\beta = \frac{s(\omega)}{p}\sqrt{\omega^2 L_R C_R + \frac{1}{\omega^2 L_L C_L} - \frac{L_R C_L + L_L C_R}{L_L C_L}} \tag{4}$$

where

$$s(\omega) = \begin{cases} -1, & \text{if } \omega < \min\left(\dfrac{1}{\sqrt{L_R C_L}}, \dfrac{1}{\sqrt{L_L C_R}}\right) \\ 1, & \text{if } \omega > \max\left(\dfrac{1}{\sqrt{L_R C_L}}, \dfrac{1}{\sqrt{L_L C_R}}\right). \end{cases} \tag{5}$$

Initially, the goal is to design a balanced CRLH unit cell with $C_R = C_L = 2$ pF, $L_R = L_L = 5.4$ nH to have a center frequency of 1.55 GHz shown in Fig. 4. However, when the active part is loaded, we anticipate an increase in C_R due to the drain-to-source capacitor of the FETs. Therefore, to obtain a better estimation of β_d in the fabricated prototype, we consider C_R to be 2.5 pF.

Fig. 5 depicts the normalized IF power at Port 2 in the transmit and receive modes based on (1) for RF = 2 GHz. As can be observed, when LO is around 3 GHz, not only the IF power reaches its maximum at Port 2 but also the isolation more than 10 dB can be clearly seen between the transmit and receive modes as shown in Fig. 5. While we only illustrate the isolation at RF = 2 GHz, it is observed that good isolation can be achieved across all the RF signals in the fast wave region by adjusting the LO signal to obtain an IF ranging from 0.9 to 1.1 GHz.

In practical scenarios, the CRLH LWA on the drain line receives the RF signal, while the large LO signal modulates

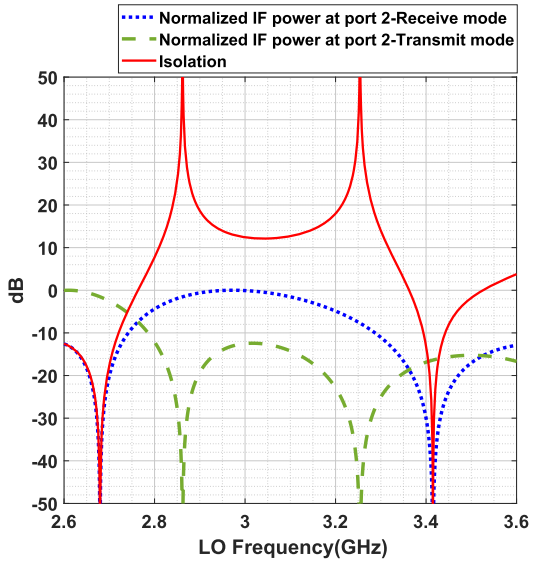

Fig. 5. Normalized IF power at Port 2 in receive and transmit modes calculated based on (1) and their difference (Isolation) when RF = 2 GHz.

the drain capacitor of the FETs. The mixing of these signals generates the IF signal, which propagates along the drain line and delivers IF power at both the ends. For the transmit mode, the downconverted IF generated at the ith unit cell (the first unit cell from the right side is considered as $i = 1$) can be written as

$$\begin{aligned} V_i^{\mathrm{Tx}}(t) &= V_i^{\mathrm{LO}}(t) * V_i^{\mathrm{RF}}(t) \\ &= \cos\big((\omega_c - \omega_{\mathrm{RF}})t - p\big(i\beta_g(f_{\mathrm{LO}}) - (N-i)\beta_d(f_{\mathrm{RF}})\big)\big) \end{aligned} \tag{6}$$

$$V_i^{\mathrm{LO}}(t) = \cos\big(\omega_c t - ip\beta_g(f_{\mathrm{LO}})\big) \tag{7}$$

$$V_i^{\mathrm{RF}}(t) = \cos(\omega_{\mathrm{RF}} t - (N-i)p\beta_d(f_{\mathrm{RF}})) \tag{8}$$

where $V_i^{\mathrm{LO}}(t)$ and $V_i^{\mathrm{RF}}(t)$ are the LO and RF signals reaching at the ith unit cell, respectively. ω_c is the LO frequency, ω_{RF} is the RF frequency, $\beta_g(f_{\mathrm{LO}})$ is the propagation constant of gate line at the LO frequency, in which the gate line is a nondispersive microstrip line, $\beta_d(f_{\mathrm{RF}})$ is the drain line propagation constant at the RF frequency, N is the number of cells, and p is the CRLH unit cell length.

The total modulated signal arriving at the right end (Port 2) is given by

$$\begin{aligned} V_{\mathrm{Right}}^{\mathrm{Tx}}(t) &= \sum_{i=1}^{N} V_i^{\mathrm{Tx}}\left(t - \frac{ip\beta_d(f_{\mathrm{IF}})}{\omega_c - \omega_{\mathrm{RF}}}\right) \\ &= \sum_{i=1}^{N} \cos\big((\omega_c - \omega_{\mathrm{RF}})t \\ &\qquad - p\big(i\beta_g(f_{\mathrm{LO}}) - (N-i)\beta_d(f_{\mathrm{RF}}) \\ &\qquad + i\beta_d(f_{\mathrm{IF}})\big)\big). \end{aligned} \tag{9}$$

For simplicity, the mixing gain is assumed to be unity as the absolute value of conversion gain/loss is irrelevant to the directional isolation performance. In the receive mode, supposing that the RF signal is illuminated to the antenna at the main beam angle, each unit cell receives the RF signal, traveling toward the Port 1. After the reception of the signal by the nth CRLH unit cell, the generated downconverted IF

at the ith unit cell can be written as

$$V_i^{\mathrm{Rx}}(t) = V_i^{\mathrm{LO}}(t) * V_i^{\mathrm{RF}}(t) = a\cos\big((\omega_c-\omega_{\mathrm{RF}})t - p\big(i\beta_g(f_{\mathrm{LO}}) - (i-n)\beta_d(f_{\mathrm{RF}})\big) - \varphi_n\big), \quad \text{for } i = n,\ n+1,\ldots,N \tag{10}$$

where

$$V_i^{\mathrm{LO}}(t) = \cos\big(\omega_c t - ip\beta_g(f_{\mathrm{LO}})\big) \tag{11}$$

$$V_i^{\mathrm{RF}}(t) = b\cos(\omega_{\mathrm{RF}}t - (i-n)\beta_d(f_{\mathrm{RF}}) + \varphi_n) \tag{12}$$

$$\varphi_n = (N-n)\frac{2\pi}{\lambda_0}p\cdot\sin\theta_0 = (N-n)p\beta_d(f_{\mathrm{RF}}) \tag{13}$$

$$\theta_0 = \arcsin\left(\frac{\beta_d(f_{\mathrm{RF}})}{k_0}\right) \tag{14}$$

with $i \geq n$, since the signal received by the nth unit cell will travel to the left side (Port 1). b is the amplitude of the received signal by each CRLH unit cell. The modulated signal arriving at the right end (Port 2) is given by

$$V_{n\_\mathrm{Right}}^{\mathrm{Rx}}(t) = \sum_{i=1}^{N} V_i^{\mathrm{Rx}}\left(t - \frac{ip\beta_d(f_{\mathrm{IF}})}{\omega_c-\omega_{\mathrm{RF}}}\right) = \sum_{i=n}^{N} b\cos\big((\omega_c-\omega_{\mathrm{RF}})t - p\big(i\beta_g(f_{\mathrm{LO}}) - (i-n)\beta_d(f_{\mathrm{RF}}) + i\beta_d(f_{\mathrm{IF}})\big) - \varphi_n\big). \tag{15}$$

Therefore, the total modulated signal arriving at the right end when all the unit cells receive the RF signal simultaneously can be written as

$$V_{\mathrm{Right}}^{\mathrm{Rx}}(t) = \sum_{n=1}^{N} V_{n\_\mathrm{Right}}^{\mathrm{Rx}}(t) = \sum_{n=1}^{N}\sum_{i=n}^{N} b\cos\big((\omega_c-\omega_{\mathrm{RF}})t - p\big(i\beta_g(f_{\mathrm{LO}}) - (i-n)\beta_d(f_{\mathrm{RF}}) + i\beta_d(f_{\mathrm{IF}})\big) - \varphi_n\big). \tag{16}$$

For simplicity, in the rest of derivations, only the positive frequency terms will be considered without loss of generality. The isolation between the transmit mode and the receive mode with respect to the downconverted IF at Port 2 can thus be defined as follows:

$$\text{Isolation} = \left|\frac{b\sum_{n=1}^{N}\sum_{i=n}^{N} e^{j\left(\left(-p\left(i\beta_g(f_{\mathrm{LO}})-(i-n)\beta_d(f_{\mathrm{RF}})+i\beta_d(f_{\mathrm{IF}})\right)-\varphi_n\right)\right)}}{\sum_{i=1}^{N} e^{-jp\left(i\beta_g(f_{\mathrm{LO}})-(N-i)\beta_d\left(f_{\mathrm{RF}}\right)+i\beta_d(f_{\mathrm{IF}})\right)}}\right|. \tag{17}$$

Substituting (13) into the above expression and considering $|e^{j\varphi}| = 1$, yield

$$\text{Isolation} = \left|\frac{be^{-jpN\beta_d(f_{\mathrm{RF}})}\sum_{n=1}^{N}\sum_{i=n}^{N} e^{-jpi\left(\beta_g(f_{\mathrm{LO}})-\beta_d(f_{\mathrm{RF}})+\beta_d(f_{\mathrm{IF}})\right)}}{e^{jpN\beta_d(f_{\mathrm{RF}})}\sum_{i=1}^{N} e^{-jpi\left(\beta_g(f_{\mathrm{LO}})+\beta_d(f_{\mathrm{RF}})+\beta_d(f_{\mathrm{IF}})\right)}}\right|. \tag{18}$$

Using the formula for a geometric sequence, we have

$$\text{Isolation} = \left|\frac{b\left(\frac{r^1-r^{N+1}}{1-r} + \frac{r^2-r^{N+1}}{1-r} + \cdots + \frac{r^N-r^{N+1}}{1-r}\right)}{\frac{m^1-m^{N+1}}{1-m}}\right| \tag{19}$$

where

$$r = e^{-jp\left(\beta_g(f_{\mathrm{LO}})-\beta_d(f_{\mathrm{RF}})+\beta_d(f_{\mathrm{IF}})\right)} \tag{20}$$

$$m = e^{-jp\left(\beta_g(f_{\mathrm{LO}})+\beta_d(f_{\mathrm{RF}})+\beta_d(f_{\mathrm{IF}})\right)}. \tag{21}$$

Then we have

$$\text{Isolation} = \left|\frac{b\left(\frac{\left(r-r^{N+1}\right)}{1-r} - Nr^{N+1}\right)}{\frac{m^1-m^{N+1}}{1-m}}\right| = \left|\frac{b\left(\frac{\left(1-r^{N}\right)}{1-r} - Nr^{N}\right)}{\frac{1-m^{N}}{1-m}}\right|. \tag{22}$$

Finally, we obtain

$$\text{Isolation} = b\left|\frac{\frac{\sin\left(\frac{Np\theta_r}{2}\right)}{\sin\left(\frac{p\theta_r}{2}\right)} - Ne^{\frac{-jp(N+1)\theta_r}{2}}}{\frac{\sin\left(\frac{p\theta_r}{2}\right)}{\sin\left(\frac{Np\theta_t}{2}\right)}}\right| \tag{23}$$

where

$$\theta_r = \left|\beta_g(f_{\mathrm{LO}}) - \beta_d(f_{\mathrm{RF}})\right| + \beta_d(f_{\mathrm{IF}}) \tag{24}$$

$$\theta_t = \left|\beta_g(f_{\mathrm{LO}}) + \beta_d(f_{\mathrm{RF}})\right| + \beta_d(f_{\mathrm{IF}}). \tag{25}$$

Moreover, if we need to use the calculated isolation formula for the Left-handed region of CRLH LWA with RF greater than LO, it is necessary to use absolute values in (24) and (25). For the fair comparison of the IF power at Port 2 between the transmit and receive modes, i.e., for isolation calculation, we suppose that the power received by the CRLH LWA is equal to the injected power in the transmit mode, and therefore we take $b = 1/N$. For simplicity, we ignore the loss of the signal during propagation along the drain line and the leakage from the radiation. Since such loss exists in both the transmit and receive modes, it will not have considerable effect in the isolation calculation. It is noted that good isolation can be obtained where the numerator becomes maximum or the denominator becomes minimum in (23). Since it is desired to obtain maximum IF power at Port 2 in the receive mode, the objective here is to obtain good isolation where the numerator of (23) becomes maximum. Besides, we should operate RF in the fast wave region, whereas LO and IF should be in the guided wave region of the CRLH LWA to avoid leakage at these frequencies. For example, if we choose RF = 1.9 GHz and sweep LO from 2.4 to 3.1 GHz to have LO and IF in the guided wave region, the normalized IF power in the receive and transmit modes, i.e., the numerator and denominator of (23), and the calculated isolation can be obtained as shown in Fig. 6. Fig. 7 depicts the results for RF = 1.3 GHz which is in the left-handed region. When RF is 1.9 GHz, it can be seen that the maximum of IF power at Port 2 in the receive mode occurs when LO = 2.8 GHz. In addition, the minimum amount of IF power at this port in the transmit mode with LO = 2.8 GHz is obtained as well. On the other hand, when RF is

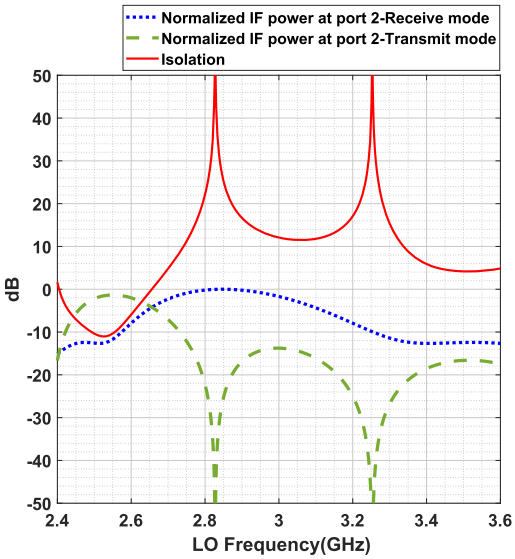

Fig. 6. Normalized IF power in the receive and transmit modes and calculated isolation based on (23) when RF = 1.9 GHz.

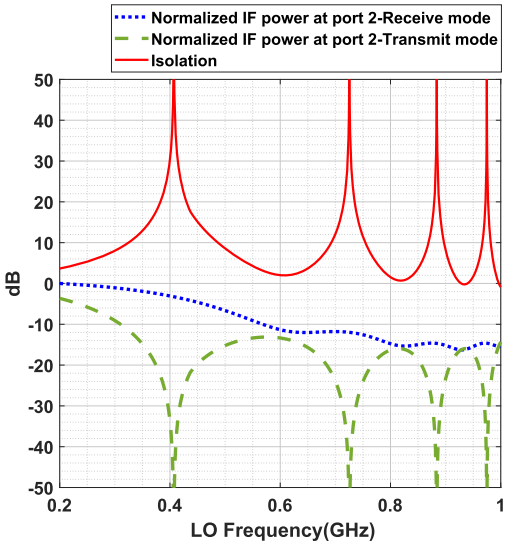

Fig. 7. Normalized IF power in the receive and transmit modes and calculated isolation based on (23) when RF = 1.3 GHz.

1.3 GHz (left-handed region), good isolation can be observed when LO = 0.4 GHz. By investigating the isolation versus LO frequency for various RF frequencies in the fast wave region, we noticed that when we take IF = 0.9 GHz, a good isolation can be obtained in all the RF frequencies in the right- and left-handed regions. However, for RF frequencies in the right-handed region, by choosing IF = 1 and 1.1 GHz, good isolation can still be achieved. We need to clarify that for the RF in the right-handed region, 1.5 GHz < RF < 2.4 GHz, we take IF = LO − RF, and for the RF in the left-handed region, 1.2 GHz < RF < 1.5 GHz, we have IF = RF − LO.

The generated upconverted IF for RF frequencies in the RH region is greater than the cutoff frequency (f_C) of the balanced CRLH transmission line which can be calculated according to [27] as follows:

$$f_C = f_R\left(1+\sqrt{\frac{f_L}{f_R}}\right) \tag{26}$$

where

$$f_L = \frac{1}{2\pi\sqrt{L_L C_L}} \tag{27}$$

$$f_R = \frac{1}{2\pi\sqrt{L_R C_R}}. \tag{28}$$

In our case, based on the aforementioned unit cell parameters, the estimated cutoff frequency will be around 3.6 GHz. As such, the generated upconverted IF cannot propagate in the CRLH TL and will be suppressed.

B. Simulated Linearity Performance of DM

To analyze linearity performance, we inject the RF into Port 2 while in the receive mode, to extract information from the IF signal at this port. Initially, we plot the IF power at Port 2 by varying the RF input. Subsequently, a two-tone RF input is introduced, with $f_{\mathrm{LO}} - (2f_{\mathrm{RF1}} - f_{\mathrm{RF2}})$ and $f_{\mathrm{LO}} - (2f_{\mathrm{RF2}} - f_{\mathrm{RF1}})$ at Port 2 considered as IM3 components. The results are displayed in Fig. 8, where the interception point is identified at 16 dBm. Therefore, the structure exhibits linear behavior when the received signal power is below 5 dBm. In this simulation, the LO power is set to 10 dBm, the RF frequency to 2.1 GHz, and the LO frequency to 3.1 GHz. The two tones used are 2.099 and 2.101 GHz. This approach allows for the generation of similar plots for other RF frequencies as well.

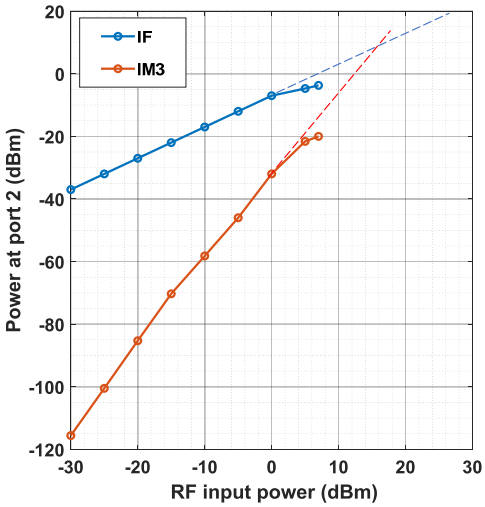

Fig. 8. Simulated linearity performance of the prototype.

III. Design and Fabrication

A. Unit Cell Design

Interdigital capacitors and shunt stub inductors are used for microstrip implementation of CRLH LWA on the drain line [27]. The center frequency of the balanced unit cell is designed to be 1.55 GHz. Intersection between the air line and dispersion diagram of CRLH unit cell determines the fast wave region which is from 1.3 to 2.3 GHz and can be seen in Fig. 4. Due to the drain–source capacitance of FETs (C_{ds}), a slight center frequency shift and band gap are expected after loading the active part. The injected RF signal will be in the fast wave region, whereas the LO and downconverted IF signal should

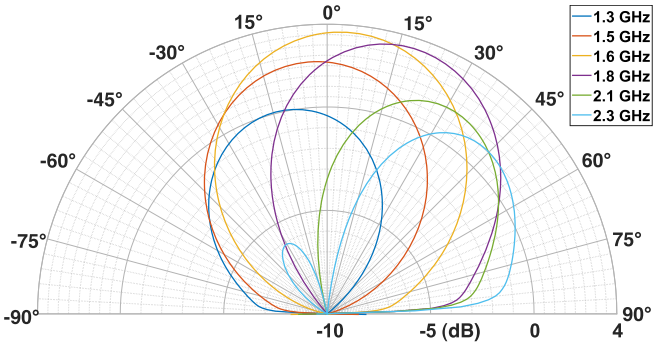

Fig. 9. Simulated gain of six cells CRLH LWA before loading active part in XZ cut.

be in the guided wave region to avoid leakage radiation of LO and IF. The LO signal is injected from the gate line which is a microstrip line. The dispersion curve of a nondispersive microstrip line by considering the dielectric constant of the substrate is also shown in Fig. 4, for comparison.

B. CRLH DM Prototype

Six cells are connected in a cascade fashion to create an LWA. Fig. 9 presents the simulated radiation pattern of CRLH LWA prior to incorporating the active components, and frequency scanning property can be seen from this figure.

The simulation results indicate that the radiation efficiency of the LWA is approximately 30%, which is attributed to the limited number of cells and resistive mixing. It is noted that our aim in this study is to demonstrate the proof-of-concept for nonreciprocity using a CRLH LWA with DM; as a result, we construct a prototype comprising only six cells, sufficient to exhibit such property.

Fig. 10, shows the fabricated prototype. It was fabricated on an RT/duroid 5870 substrate ($\varepsilon_r = 2.33$, $h = 1.57$ mm). The prototype consists of six CRLH cells in drain line of NE3509M04 transistors which are used as mixing elements. The drain is biased from the end of each shunt stub of CRLH unit cell connected to a 100-pF capacitance with $V_{\rm DS} = 0.08$ V and $V_{\rm GS} = -0.2$ V to make the FETs work as a resistive mixer. The FETs are stabilized by putting two resistors in their gates. The drain sides are connected to the CRLH unit cells, and the gates are connected to a microstrip line to create a path for LO propagation.

Based on the specifications in the datasheet of the used transistor and our measurements, when under the given bias conditions, the drain current I_D is 2 mA. As a result, the dc power consumption calculates to $6V_DI_D = 0.96$ mw. This amount is considered minimal due to the bias point necessary for resistive mixing [28].

IV. Experimental Results

A. Radiation Pattern, Isolation, and Noise Figure

First, we measure the radiation pattern of CRLH LWA after loading the mixing components to validate the beam scanning property. The normalized radiation pattern is plotted in Fig. 11. One can see the frequency-scanning capability by increasing the frequency in the fast wave region. The center frequency

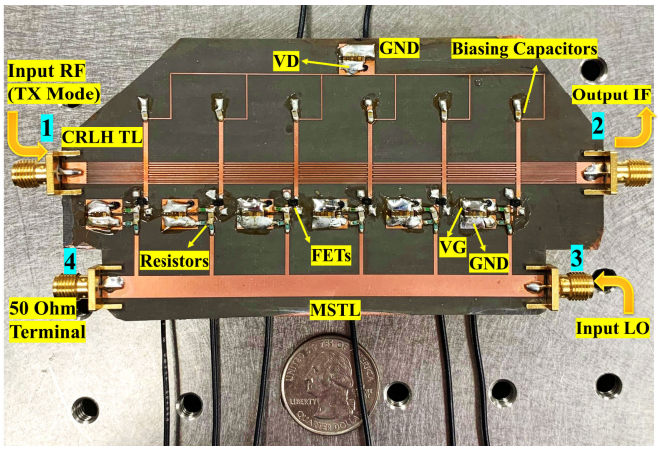

Fig. 10. Fabricated prototype of the proposed nonreciprocal CRLH metamaterial LWA based on DM.

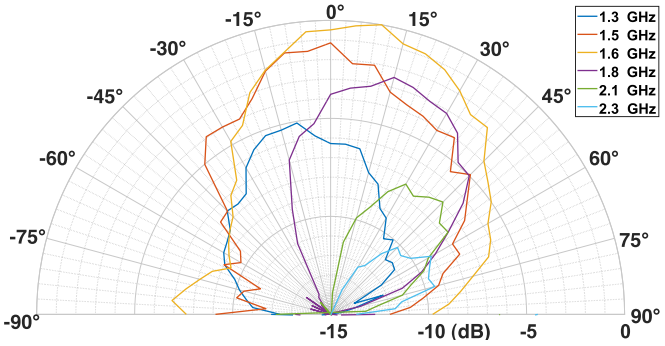

Fig. 11. Measured normalized radiation pattern of LWA after loading the active part in XZ cut.

has been shifted a bit after loading the active part. As a result, the fast wave region is from 1.2 to 2.2 GHz.

Considering the real scenario, in the receive mode, the RF power is illuminated to the DM-based CRLH LWA structure through a horn antenna. According to the Friis transmission formula, by taking into account the gains of the horn antenna and our LWA at different frequencies, and the distance between them equal to the minimum possible distance such that the antenna operates in the far-field region, the maximum power can be received by the prototype is around -30 dBm. Therefore, to have a fair calculation for isolation, we inject -30 dBm from Port 1 in the transmit mode with an LO power equal to 8 dBm. The isolation is calculated as follows:

$$\text{Isolation(dB)} = P_{\text{IF}-\text{Receice Mode at Port 2}}(\text{dBm}) - P_{\text{IF}-\text{Transmit Mode at Port 2}}(\text{dBm}). \quad (29)$$

Fig. 12 depicts the measured conversion loss when IF = 1 GHz. Besides, the simulation results are plotted while the RF power is injected into Port 2. For IF = 0.9 and 1.1 GHz, conversion loss changes between 6 and 12 dB. Fig. 13 illustrates the results of the calculated [based on (23)] and measured isolation for IF = 0.9 and 1.1 GHz, where the measurement setup for the receive mode is shown in Fig. 14. The small center frequency shift has been considered in the dispersion diagram of CRLH unit cell for the calculation of isolation. The results shown in Fig. 13 verify the good isolation when IF is 0.9 GHz or 1.1 GHz. As can be seen in Figs. 6 and 7, the IF power in the transmit mode shows sharp resonances,

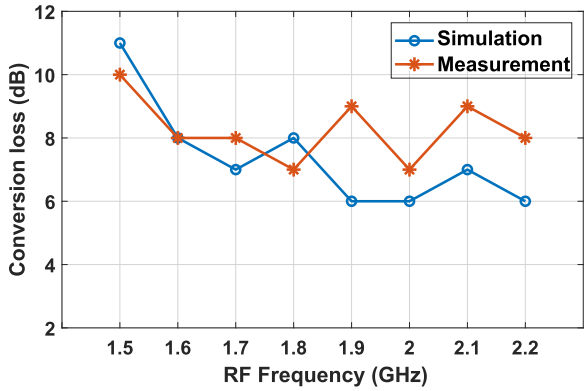

Fig. 12. Simulated and measured conversion losses when IF = 1 GHz.

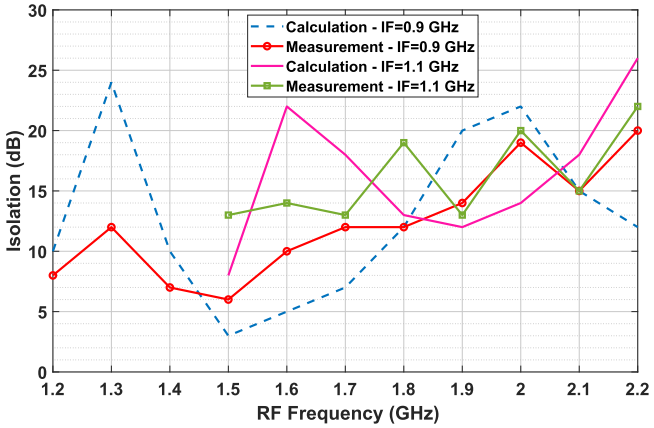

Fig. 13. Calculated and measured isolation.

in which a little shift from these resonant frequencies will lead to difference in the isolation. In practice, it is more likely that in the fabricated prototype, the resonant frequencies are not exactly where we expect based on the calculation which may be the reason for the difference between the calculated and measured isolation.

Fig. 15 illustrates the simulated and measured noise figures of the mixer in the receive mode. Since simulating or measuring the noise figure is not feasible when the signal illuminates the DM in the receive mode, the results are obtained by injecting the signal into Port 2, which is also considered as the output port. The measurement setup is depicted in Fig. 16. Given the conversion loss shown in Fig. 12 for a resistive FET mixer, the plotted results for the noise figure are anticipated. On the other hand, active mixing can be leveraged to further reduce the noise figure.

B. Simultaneous Transmit and Receive Operation

To showcase the concurrent capabilities of transmission and reception, a measurement setup involving three universal software radio peripherals (USRPs) is conducted, as illustrated in Figs. 17 and 18. The setup uses GNU Radio software to enact the IEEE 802.11 standard for transmitting and receiving orthogonal frequency-division multiplexing (OFDM) packets with both QPSK and 16QAM modulation schemes. A single-frequency LO signal is fed into Port 3 of the fabricated DM, while an OFDM signal functioning as the RF with a center frequency of 1.3 GHz and 64 subcarriers is injected to Port 1 through USRP 1 as the transmitted signal. Concurrently,

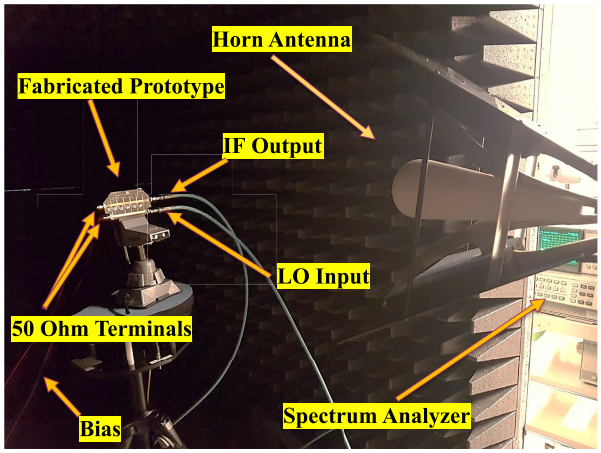

Fig. 14. Measurement setup for the receive mode.

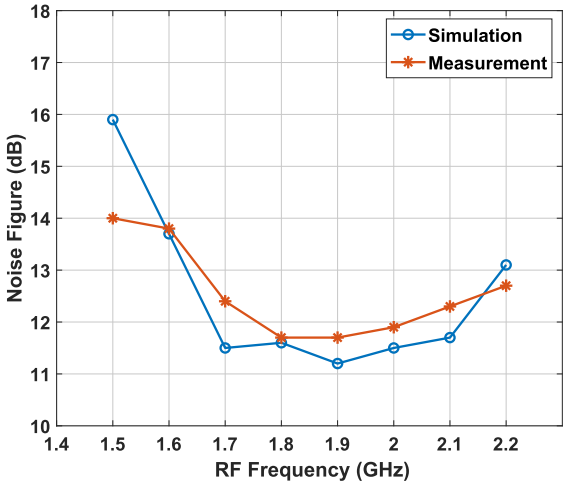

Fig. 15. Simulated and measured noise figures when IF = 1 GHz.

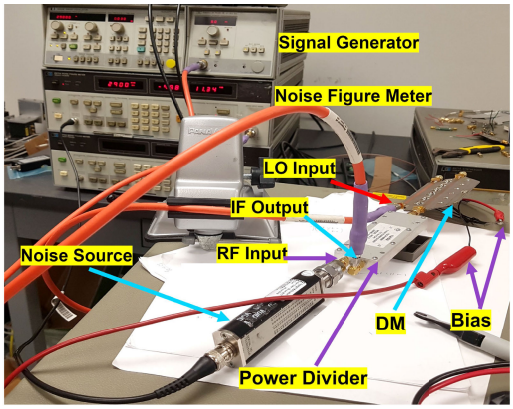

Fig. 16. Noise figure measurement setup.

USRP 2 generates another OFDM signal, which is then broadcast to the prototype using a horn antenna. USRP 3, linked to Port 2 of the DM, captures information at an IF signal. Considering that the antenna receives power at approximately −25 dBm at the RF frequency in the reception mode, the same −25 dBm is injected into Port 1 for the transmission mode. Moreover, we adjust the LO frequency, as depicted in Fig. 19, to determine the frequency at which the IF power significantly decreases in the transmit mode. It is observed that there is a shift in the anticipated null point frequency

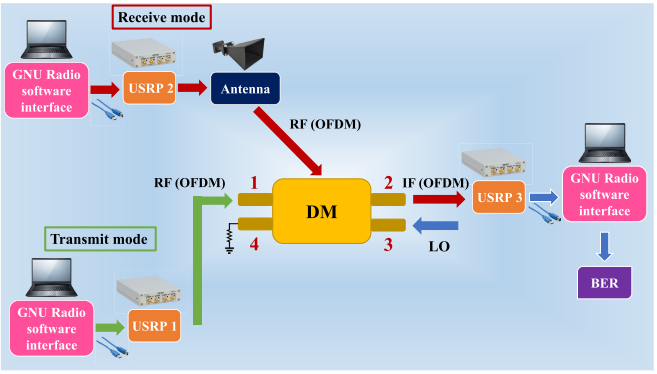

Fig. 17. Simultaneous transmit and receive measurement setup diagram.

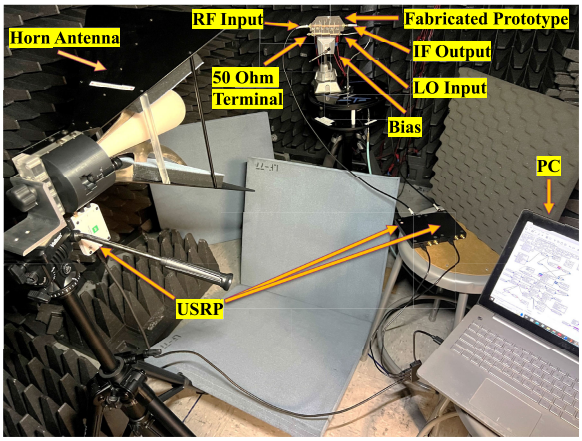

Fig. 18. Simultaneous transmit and receive measurement setup in the anechoic chamber.

based on the simulation results. Considering this, we choose LO = 0.35 GHz to achieve the optimal isolation. Figs. 20 and 21 display the constellation maps of the demodulated signal at the IF frequency, extracted from Port 2. In Fig. 20, where QPSK modulation is leveraged, the error vector magnitude (EVM_{rms}) is calculated as 0.28, and for Fig. 21 with 16QAM modulation, its EVM_{rms} is 0.20. It is noted that EVM_{rms} is calculated using the following formula [29]:

$$\mathrm{EVM_{rms}} = \sqrt{\frac{\frac{1}{T}\sum_{t=1}^{T}\left(\left|I_t - I_{0,t}\right|^2 + \left|Q_t - Q_{0,t}\right|^2\right)}{\frac{1}{M}\sum_{m=1}^{M}\left(\left|I_{0,m}\right|^2 + \left|Q_{0,m}\right|^2\right)}} \tag{30}$$

where I_t and $I_{0,t}$ stand for the normalized in-phase voltages for the measured symbols and ideal transmitted symbols in the constellation, respectively. Moreover, Q_t and $Q_{0,t}$ represent the normalized quadrature voltages for the measured symbols and ideal transmitted symbols in the constellation, respectively. M denotes the number of unique symbols in the constellation and T denotes the total number of symbols in the constellation (typically $T \gg M$).

In addition, by comparing the bits of the received packets through USRP 3 with the sent bits through USRP 2, BER can be calculated. With a set illuminated RF power, we vary the injected power in the transmit mode and measure the BER, as shown in Fig. 22. When the power received by the prototype closely matches the transmitted power level, a satisfactory BER is maintained for both the modulation schemes. This allows for effective data extraction from Port 2 of the DM at the IF frequency. Furthermore, at a fixed RF frequency,

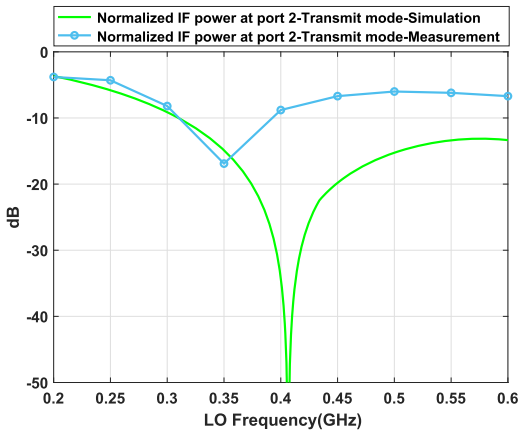

Fig. 19. Normalized IF power at Port 2 when RF = 1.3 GHz.

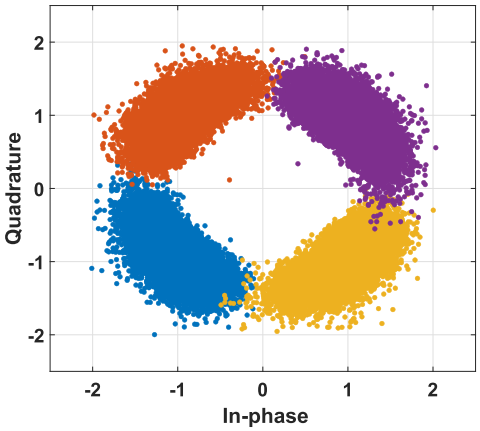

Fig. 20. Constellation map of the received signal with QPSK modulation when RF = 1.3 GHz and LO = 0.35 GHz.

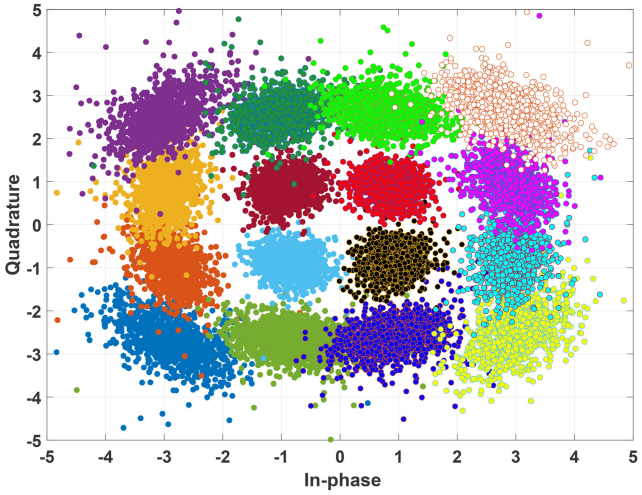

Fig. 21. Constellation map of the received signal with 16QAM modulation when RF = 1.3 GHz and LO = 0.35 GHz.

by fine-tuning the LO frequency to align with the precise null point, an acceptable BER can be achieved using QPSK modulation, even when the transmitted RF power exceeds the received RF power at the prototype by 10 dB. Moreover, it is evident that QPSK modulation offers superior transmission reliability, although at the cost of lower spectral efficiency compared with 16QAM modulation. To enhance the BER for a robust system, one can use high modulation grades with increased number of redundant bits which enable recovering the original information. Besides, the illuminated power needs to be increased to ensure greater isolation.

TABLE I
COMPARISON OF THE PROPOSED FULL-DUPLEX ANTENNA WITH RELATED WORKS

Ref.	Size (λ_0^3)	Frequency (GHz)	Mixing	Isolation(dB)	OTA BER* measurement
[30]	$2.67 \times 0.40 \times 0.02$	5.85 – 6.1	No	17	No
[31]	$11.7 \times 11.7 \times 0.3$	27.6 – 29.5	No	55	No
[32]	$0.25 \times 0.25 \times 0.04$	2.4 – 2.52	No	25	No
[33]	$0.45 \times 0.20 \times 0.04$	3.4 – 3.8	No	45	No
[34]	$0.37 \times 0.37 \times 0.08$	0.912 - 0.934	No	30	No
[25]	$1.5 \times 0.4 \times 0.02$	1.88 - 2	Yes	30	No
This work	$\mathbf{0.65 \times 0.31 \times 0.01}$	**1.3 – 2.2**	**Yes**	**22**	**Yes**

* Over-the-air bit-error-rate

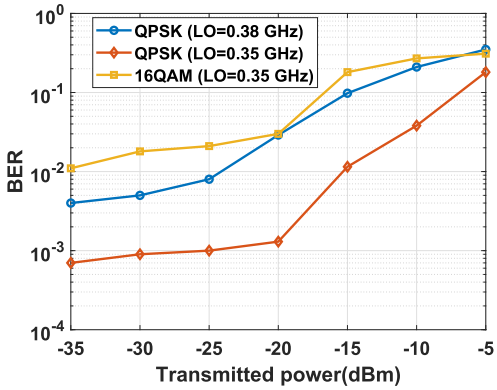

Fig. 22. Measured BER result for a fixed illuminated power while sweeping the injected power at Port 1 (transmitted power).

Our proposed antenna uses mixing to achieve full-duplex functionality, setting it apart from traditional full-duplex antennas. A comparison of our design with other documented efforts in the field is shown in Table I. Notably, despite its comparatively short length, the proposed design effectively ensures sufficient isolation for full-duplex operations. In addition, we explore the capability for simultaneous transmission and reception by performing OTA BER measurements.

V. CONCLUSION

This study presents a CRLH nonreciprocal LWA, designed based on the distributed mixing principle for concurrent transmission and reception. The LO signal, fed through the gate line, combines with the RF signal in the fast wave region of the CRLH LWA. This combination yields a downconverted IF at the reverse port, displaying variable conversion gains for both transmitting and receiving. Notably, at certain IF frequencies, the reverse port on the drain line achieves significant isolation due to CRLH DM's direction-dependent mixing characteristic. This design enhances the extraction of data from the downconverted IF signal in the reception mode. A six-cell prototype of this system has been developed, demonstrating effective isolation at selected IF frequencies, corroborating our theoretical analysis that links isolation with the downconverted IF signal in the proposed CRLH DM.

REFERENCES

[1] O. San A. Tang and C. S. Aitchison, "A very wide-band microwave MESFET mixer using the distributed mixing principle," *IEEE Trans. Microw. Theory Techn.*, vol. MMT-33, no. 12, pp. 1470–1478, Dec. 1985.

[2] O. S. A. Tang and C. S. Aitchison, "A microwave distributed MESFET mixer," in *Proc. 14th Eur. Microw. Conf.*, Oct. 1984, pp. 483–487.

[3] A. Q. Safarian, A. Yazdi, and P. Heydari, "Design and analysis of an ultrawide-band distributed CMOS mixer," *IEEE Trans. Very Large Scale Integr. (VLSI) Syst.*, vol. 13, no. 5, pp. 618–629, May 2005.

[4] K.-L. Deng and H. Wang, "A 3–33 GHz PHEMT MMIC distributed drain mixer," in *IEEE Radio Freq. Integr. Circuits (RFIC) Symp. Dig. Papers*, Jun. 2002, pp. 151–154.

[5] A. Nooraiepour, S. Vosoughitabar, C.-T.-M. Wu, W. U. Bajwa, and N. B. Mandayam, "Programming wireless security through learning-aided spatiotemporal digital coding metamaterial antenna," *Adv. Intell. Syst.*, vol. 5, no. 10, Oct. 2023, Art. no. 2300341.

[6] S. Vosoughitabar and C.-T.-M. Wu, "Programming nonreciprocity and harmonic beam steering via a digitally space-time-coded metamaterial antenna," *Sci. Rep.*, vol. 13, no. 1, p. 7338, May 2023.

[7] A. Nooraiepour, S. Vosoughitabar, C.-T.-M. Wu, W. U. Bajwa, and N. B. Mandayam, "Time-varying metamaterial-enabled directional modulation schemes for physical layer security in wireless communication links," *ACM J. Emerg. Technol. Comput. Syst.*, vol. 18, no. 4, pp. 1–20, Oct. 2022, doi: 10.1145/3513088.

[8] S. Vosoughitabar, A. Nooraiepour, W. U. Bajwa, N. Mandayam, and C. T. M. Wu, "Metamaterial-enabled 2D directional modulation array transmitter for physical layer security in wireless communication links," in *IEEE MTT-S Int. Microw. Symp. Dig.*, Jun. 2022, pp. 595–598.

[9] J. Mata-Contreras, C. Camacho-Penalosa, and T. M. Martin-Guerrero, "Active distributed mixers based on composite Right/Left-handed transmission lines," *IEEE Trans. Microw. Theory Techn.*, vol. 57, no. 5, pp. 1091–1101, May 2009.

[10] C. M. Wu and T. Itoh, "Wideband/image-rejection distributed mixer integrated with a CRLH leaky wave antenna," in *Proc. Asia–Pacific Microw. Conf.*, Dec. 2010, pp. 634–637.

[11] P. de Paco, R. Villarino, G. Junkin, O. Menendez, E. Corrales, and J. Parron, "Dual-band mixer using composite right/left-handed transmission lines," *IEEE Microw. Wireless Compon. Lett.*, vol. 17, no. 8, pp. 607–609, Aug. 2007.

[12] J. Mata-Contreras, T. M. Martin-Guerrero, and C. Camacho-Penalosa, "Assessment of a composite right/left-handed transmission line-based distributed amplifier implemented in microstrip technology," in *Proc. Eur. Microw. Conf.*, Sep. 2006, pp. 1586–1589.

[13] C. M. Wu, Y. Dong, J. S. Sun, and T. Itoh, "Ring-resonator-inspired power recycling scheme for gain-enhanced distributed amplifier-based CRLH-transmission line leaky wave antennas," *IEEE Trans. Microw. Theory Techn.*, vol. 60, no. 4, pp. 1027–1037, Apr. 2012.

[14] C.-T. Michael Wu and T. Itoh, "A re-radiating CRLH-transmission line leaky wave antenna using distributed amplifiers," in *Proc. Asia Pacific Microw. Conf.*, Singapore, Dec. 2009, pp. 1998–2001.

[15] C. M. Wu and T. Itoh, "Dual-fed distributed amplifier-based CRLH-leaky wave antenna for gain-enhanced power combining," in *IEEE MTT-S Int. Microw. Symp. Dig.*, May 2012, pp. 87–90.

[16] C. M. Wu and T. Itoh, "Combined gain-enhanced power recycling feedbacks for distributed amplifier-based CRLH-leaky wave antennas," in *Proc. 41st Eur. Microw. Conf.*, Oct. 2011, pp. 499–502.

[17] C. M. Wu and T. Itoh, "Gain-enhanced distributed amplifier-based CRLH-leaky wave antenna for quasi-resonant power recycling scheme," in *IEEE MTT-S Int. Microw. Symp. Dig.*, Jun. 2011, pp. 1–4.

[18] C. M. Wu and T. Itoh, "CRLH-transmission line leaky wave antennas integrated with distributed amplifiers with power recycling feedback scheme," in *Proc. 5th Eur. Conf. Antennas Propag. (EUCAP)*, Apr. 2011, pp. 3901–3904.

[19] K. Mori and T. Itoh, "Distributed amplifier with CRLH-transmission line leaky wave antenna," in *Proc. 38th Eur. Microw. Conf.*, Oct. 2008, pp. 686–689.

[20] S. Qin, Q. Xu, and Y. E. Wang, "Nonreciprocal components with distributedly modulated capacitors," *IEEE Trans. Microw. Theory Techn.*, vol. 62, no. 10, pp. 2260–2272, Oct. 2014.

[21] Y. S. Li, X. P. Yu, and Z. H. Lu, "Nonreciprocal time-varying transmission line with carrier boosting technique for low-noise RF front ends," *IEEE Microw. Wireless Compon. Lett.*, vol. 28, no. 11, pp. 1011–1013, Nov. 2018.

[22] G. Buchta, "Magnetically scanned reciprocal and nonreciprocal leaky-wave antennas," *Proc. IEEE*, vol. 52, no. 5, pp. 625–626, May 1964.

[23] N. Apaydin, K. Sertel, and J. L. Volakis, "Nonreciprocal leaky-wave antenna based on coupled microstrip lines on a non-uniformly biased ferrite substrate," *IEEE Trans. Antennas Propag.*, vol. 61, no. 7, pp. 3458–3465, Jul. 2013.

[24] N. Apaydin, L. Z. Lee, K. Sertel, and J. L. Volakis, "Nonreciprocal and magnetically scanned leaky-wave antenna using coupled CRLH lines," in *Proc. IEEE Antennas Propag. Soc. Int. Symp. (APSURSI)*, Jul. 2013, pp. 2297–2298.

[25] S. Taravati and C. Caloz, "Mixer-duplexer-antenna leaky-wave system based on periodic space-time modulation," *IEEE Trans. Antennas Propag.*, vol. 65, no. 2, pp. 442–452, Feb. 2017.

[26] S. Vosoughitabar, M. Zhu, and C. M. Wu, "A distributed mixer-based nonreciprocal CRLH leaky wave antenna for simultaneous transmit and receive," in *IEEE MTT-S Int. Microw. Symp. Dig.*, Jun. 2021, pp. 408–411.

[27] T. Itoh and C. Caloz, *Electromagnetic Metamaterials: Transmission Line Theory and Microwave Applications*. Hoboken, NJ, USA: Wiley, 2005.

[28] CEL. *NE3509M04 Datasheet*. Accessed: Jul. 12, 2020. [Online]. Available: https://www.mouser.com/datasheet/2/286/ne3509m04-19679.pdf

[29] R. A. Shafik, M. S. Rahman, and A. R. Islam, "On the extended relationships among EVM, BER and SNR as performance metrics," in *Proc. Int. Conf. Electr. Comput. Eng.*, Dec. 2006, pp. 408–411.

[30] T. Kodera and C. Caloz, "Integrated leaky-wave antenna–duplexer/diplexer using CRLH uniform ferrite-loaded open waveguide," *IEEE Trans. Antennas Propag.*, vol. 58, no. 8, pp. 2508–2514, Aug. 2010.

[31] Q.-C. Ye, Y.-M. Zhang, J.-L. Li, G. F. Pedersen, and S. Zhang, "High-isolation dual-polarized leaky-wave antenna with fixed beam for full-duplex millimeter-wave applications," *IEEE Trans. Antennas Propag.*, vol. 69, no. 11, pp. 7202–7212, Nov. 2021.

[32] Y. He and Y. Li, "Compact co-linearly polarized microstrip antenna with fence-strip resonator loading for in-band full-duplex systems," *IEEE Trans. Antennas Propag.*, vol. 69, no. 11, pp. 7125–7133, Nov. 2021.

[33] Z. Wang, T. Liang, and Y. Dong, "Compact in-band full duplexing antenna for sub-6 GHz 5G applications," *IEEE Antennas Wireless Propag. Lett.*, vol. 20, pp. 683–687, 2021.

[34] D. Inserra and G. Wen, "Dual orthogonal port stacked patch antenna with vertical pins for simultaneous transmit and receive application," *IEEE Trans. Antennas Propag.*, vol. 69, no. 12, pp. 8908–8913, Dec. 2021.

Shaghayegh Vosoughitabar (Graduate Student Member, IEEE) received the B.S. and M.S. degrees in electrical engineering from Iran University of Science and Technology (IUST), Tehran, Iran, in 2017 and 2020, respectively. She is currently pursuing the Ph.D. degree in electrical and computer engineering at Rutgers, The State University of New Jersey, New Brunswick, NJ, USA.

She is working as a Research Assistant with the Microwave Research Laboratory Rutgers, The State University of New Jersey. Her research interests include metamaterials, RF circuit, and antenna design for wireless communication.

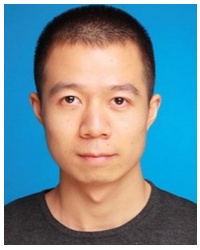

Minning Zhu (Member, IEEE) received the B.S. degree in optical information science and technology from Harbin Institute of Technology, Harbin, Heilongjiang, China, in 2010, the M.S. degree in optics from Shanghai University, Shanghai, China, in 2014, and the Ph.D. degree in electrical and computer engineering from Rutgers, The State University of New Jersey, New Brunswick, NJ, USA, in 2021.

Since September 2021, he has been a Post-Doctoral Researcher with the Microwave Research Laboratory (MWLab), ECE, Rutgers. He has published works on journals such as IEEE TRANSACTIONS ON MICROWAVE THEORY AND TECHNIQUES (TMTT), *Journal of the Optical Society of America A* (JOSAA), and *Optics Express*, and conference papers on IMS, EuMC, AMPC, CLEO, and is a reviewer for several journals. His research interests include applied electromagnetics, antennas, passive/active components, metamaterials, RF near/in-sensor analog computing, optical imaging, and nanofocusing.

Dr. Zhu is a member of the IEEE Microwave Theory and Techniques Society (IEEE MTT-S) and the IEEE Young Professionals Society.

Alireza Nooraiepour received the B.S. degree in electrical engineering from Amirkabir University of Technology (Tehran Polytechnic), Tehran, Iran, in 2013, the M.S. degree in electrical and electronics engineering from Bilkent University, Ankara, TÜrkiye, in 2016, and the Ph.D. degree in electrical and computer engineering from Rutgers University, New Brunswick, NJ, USA, in 2022.

He is currently a Senior Engineer with the Department of Research and Development, Qualcomm Inc., San Diego, CA, USA. His current research focuses on 5G NR wireless communications, positioning, and physical layer security.

Chung-Tse Michael Wu (Senior Member, IEEE) received the B.S. degree in electrical engineering from National Taiwan University (NTU), Taipei, Taiwan, in 2006, and the M.S. and Ph.D. degrees in electrical engineering from the University of California at Los Angeles (UCLA), Los Angeles, CA, USA, in 2009 and 2014, respectively.

From September 2008 to June 2014, he was a Graduate Student Researcher with the Microwave Electronics Laboratory, UCLA. In 2009, he was a Summer Intern with Bell Laboratories, Murray Hill, NJ, USA. In 2012, he was a Special-Joint Researcher with the Japan Aerospace Exploration Agency (JAXA), Sagamihara, Japan. From 2014 to 2017, he was an Assistant Professor with the Department of Electrical and Computer Engineering, Wayne State University (WSU), Detroit, MI, USA. In 2017, he joined Rutgers University, New Brunswick, NJ, USA, as an Assistant Professor and was promoted to tenured Associate Professor in 2022. Since 2024, he has been an Associate Professor with NTU. His research interests include applied electromagnetics, antennas, passive/active microwave and millimeter-wave components, RF systems, and metamaterials.

Dr. Wu is a member of the Technical Committee for IEEE MTT-28 and MTT-4. He was a recipient of the National Science Foundation (NSF) Faculty Early Career Development (CAREER) Award, the WSU College of Engineering Faculty Research Excellence Award in 2016, the Defense Advanced Research Projects Agency (DARPA) Young Faculty Award (YFA) in 2019, and DARPA Director's Fellowship Award in 2021. In 2022, he was also awarded the Board of Trustees Research Fellowship for Scholarly Excellence at Rutgers University. He is also the Vice Chair for the joint AP/ED/MTT chapter of the IEEE Princeton Central Jersey Section. He currently serves as an Associate Editor for the IEEE MICROWAVE AND WIRELESS TECHNOLOGY LETTERS, the IEEE JOURNAL OF ELECTROMAGNETICS, RF AND MICROWAVES IN MEDICINE AND BIOLOGY, and IEEE ACCESS.